A Referenced Geometry Based Configuration Scalable Mextram Model for Bipolar Transistors

Hsien-Chang Wu, Slobodan Mijalkovic and Joachim N. Burghartz

Laboratory of High Frequency Technology and Components (HiTeC)
Delft University of Technology, Mekelweg 4, 2628 CD Delft, the Netherlands

Abstract — **A behavioral reference based model for configuration scaling of bipolar transistor model parameters is proposed. The model is applicable to bipolar technologies with one or two collector contacts and different number of emitters. The effectiveness of the proposed scaling methodology is verified in case studies using advanced high-speed SiGe HBT technology.**

Index Terms — **Geometry scaling, Multi-emitter SiGe HBT, Mextram model, thermal resistance, collector resistance.**

I. INTRODUCTION

With the coming era of System-on-a-Chip (SoC) there is an ever increasing number of microcircuit and system integrated in a single chip. In order to meet the increasing complexity of the circuit design, a geometry scalable model is crucial for different function blocks in SoC design. However, simple dimensional device scaling is not sufficient to meet all the circuit design requirements. For example, power amplifier applications require larger emitter area (A_E) to provide sufficient power output but emitter area can't be extended without limits. When device becomes large, emitter current crowding effect and distributed parasitic resistance will degrade device performance [1][2]. In order to provide high output power level without sacrificing too much of the device performance, it is common practice to employ several transistors in parallel or create Multi-Emitter Devices (MEDs) in power amplifier design. Between these two options, MEDs is preferred for power amplifier application because of its compactness in using chip area.

Advanced bipolar transistor model Mextram [3], which addresses all kinds of high current bipolar transistor effects [4][5], is especially suitable for power device application. In this paper, we would like to extend previously developed a reference based geometry scaling approach for Mextram model [6] to configuration scaling including different contact configurations and emitter numbers for optimal circuit design.

The paper is organized as follows. In Section II, scaling equations for MEDs, based on different layout configurations, are derived. The scalable model implementation and an ICCAP [7] model file for temperature and geometry parameter extraction from different layout configurations is introduced in Section III. The conclusion of this paper is in Section IV.

II. DERIVATION OF SCALING EQUATIONS FOR MULTI-EMITTER FINGER DEVICES

Fig.1 shows the layout of a multi-emitter SiGe HBT with its emitter (E) and collector (C) labeled. The electrical model parameters that describe currents and capacitances of the intrinsic device are simply scaled with the emitter-finger number while the ratio parameters are kept the same as for the Single-Emitter Device (SED). The resistances that define the current flow in the direction vertical to emitter window scale reciprocally to the number of the emitters.
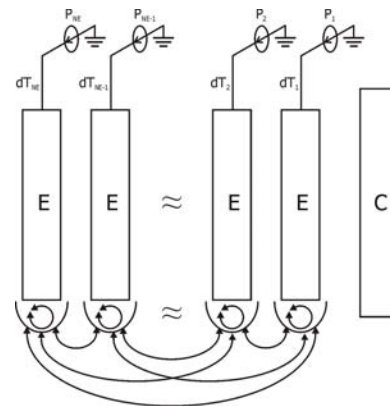
Fig. 1. Layout of a SiGe HBT structure with N_E emitters and one collector contact with self-heating and mutual-heating among emitters.

The self- and mutual-heating of emitters schematically presented in Fig. 1 produces non-uniform distribution of the temperature and in principle each emitter operates at different temperature [8]. To represent the real temperature distribution in the MED, there should be a thermal node associated with each emitter. However, Mextram is equipped with only one thermal node, which can only model the average temperature rise of the device. As a result, the temperature rise is

assumed to be uniform across the active device region, which is the region isolated by shallow trench isolation.

For each emitter, the temperature rise (dT_i) produced by the self- and mutual-heating effects can be modeled with an $N_E \times N_E$ thermal resistance matrix and its power dissipation P_i as:

$$
\begin{pmatrix} dT_1 \\ dT_2 \\ \vdots \\ dT_{N_E} \end{pmatrix} = \begin{pmatrix} Rth_{1,1} & Rth_{1,2} & \cdots & Rth_{1,N_E} \\ Rth_{2,1} & Rth_{2,2} & \cdots & Rth_{2,N_E} \\ \vdots & \vdots & \vdots & \vdots \\ Rth_{N_E,1} & Rth_{N_E,2} & \cdots & Rth_{N_E,N_E} \end{pmatrix} \begin{pmatrix} P_1 \\ P_2 \\ \vdots \\ P_{N_E} \end{pmatrix} \quad (1)
$$

The component $Rth_{i,j}$ in the thermal resistance matrix is modeled as:

$$
Rth_{i,j} = \begin{cases} Rth & i = j, \\ \dfrac{Rthc}{abs(i-j)W_D L_B} & i \neq j. \end{cases} \quad (2)
$$

where Rth and $Rthc$ are self- and mutual-heating thermal resistance parameters, W_D and L_B are the distance between two adjacent fingers and the length of the active region respectively.

The parameter Rth scales with the reciprocal area of the active region and it can be expressed as a reference based geometry scaling equation:

$$
Rth = \mathrm{RTH_R}\left(1 + \mathrm{RTHA}\left(\frac{W_B L_B}{W_{BR} L_{BR}} - 1\right)\right.
$$
$$
\left. + \mathrm{RTHW}\left(\frac{W_B}{W_{BR}} - 1\right) + \mathrm{RTHL}\left(\frac{L_B}{L_{BR}} - 1\right)\right)^{-1}. \quad (3)
$$

Where $\mathrm{RTH_R}$ is the self-heating thermal resistance at a reference geometry chosen in the available geometry matrix, W_B, W_{BR} and L_{BR} are the width, reference width and reference length of the active region. RTHA, RTHW and RTHL are the geometry parameters, which account for bulk, sidewall width and length contribution. When the device geometry is equal to the reference geometry, Rth is equal to $\mathrm{RTH_R}$. Otherwise, it scales to the evaluated geometry.

If P_i, representing the power dissipation at finger i, is assumed to be equal to the total power dissipation P divided by N_E, the average temperature rise dT in each emitter finger will be:

$$
dT = \frac{dT_1 + dT_2 \cdots dT_{N_E}}{N_E}
$$
$$
= \frac{P}{N_E^2}\left(Rth_{1,1} + Rth_{1,2} \cdots Rth_{1,N_E} + Rth_{2,1}\right.
$$
$$
\left. + Rth_{22} \cdots Rth_{2N_E} \cdots Rth_{N_E 1} + Rth_{N_E,2} \cdots Rth_{N_E,N_E}\right) \quad (4)
$$
$$
= \frac{P}{N_E}\left(Rth + \frac{2Rthc}{N_E}\sum_{i=1}^{N_E-1}\frac{N_E - i}{i W_D L_B}\right).
$$

Notice from (4), that when $N_E \geq 2$, the effective thermal resistance $RTH = dT/P$ is increased due to mutual heating effect.

From (3) and (4), the reference base scaling equations for the SED and MED's RTH, which including self- and mutual-heating thermal resistance becomes:

$$
RTH = \frac{\mathrm{RTH_R}}{N_E}\left(\left(1 + \mathrm{RTHA}\left(\frac{W_B L_B}{W_{BR}L_{BR}} - 1\right) + \mathrm{RTHW}\left(\frac{W_B}{W_{BR}} - 1\right)\right.\right.
$$
$$
\left.\left. + \mathrm{RTHL}\left(\frac{L_B}{L_{BR}} - 1\right)\right)^{-1} + \frac{2\mathrm{RTHC}}{N_E}\sum_{i=1}^{N_E-1}\frac{N_E - i}{i}\frac{W_{DR}L_{BR}}{W_D L_B}\right). \quad (5)
$$

Where RTHC is the geometry parameter for the mutual heating thermal resistance and W_{DR} is the reference geometry of W_D. If W_D has a fixed length in the process design rule, it will cancel with W_{DR}.

Similar to temperature distribution, the potential distribution along the lateral collector buried-layer of MED structure will be non-uniform because of the lateral current flow. It should be again described by a single internal collector node of the Mextram model. As a result, the total collector resistance (RCC) can only be modeled effectively. Starting from the SED with one collector contact, the RCC that comprises part of the epi-collector resistance ($Rcep$) and buried-layer resistance under epi-collector ($Rbli$), extrinsic buried-layer resistance ($Rblx$) and collector-plug resistance ($Rcpl$), as shown in Fig. 2, is expressed as:

$$
RCC = Rcep + Rbli + Rblx + Rcpl
$$
$$
= Rci + Rcx. \quad (6)
$$

where Rci is the lumped resistance of $Rcep$ and $Rbli$ and Rcx is the lumped resistance of $Rblx$ and $Rcpl$. Notice also from Fig. 2 that Rcx is modeled with its conductance at width (Gcw), length (Gcl) and corner (Gc) of the emitter as:

$$
Rcx^{-1} = GcwW_E + GclL_E + Gc. \quad (7)
$$

Thus, the reference based scaling equation for Rcx becomes:

$$
Rcx = Rcx_R\left(1 + \mathrm{GCW}\left(\frac{W_E}{W_{ER}} - 1\right) + \mathrm{GCL}\left(\frac{L_E}{L_{ER}} - 1\right)\right)^{-1}. \quad (8)
$$

where Rcx_R is the Rcx at the reference geometry. GCW and GCL are the width and length geometry parameters. The Rci is modeled with area and square of the emitter size as:

$$
Rci = Rcep + Rbli
$$
$$
= Rciv\frac{1}{W_E L_E} + Rcih\frac{W_E}{L_E}. \quad (9)
$$

Where $Rciv$ and $Rcih$ are the constant geometry parameters for $Rcep$ and $Rbli$. From (9), the reference based scaling equation of Rci becomes:

$$Rci = Rci_R\left(RCI\frac{W_{ER}L_{ER}}{W_E L_E} + (1-RCI)\frac{W_E L_{ER}}{L_E W_{ER}}\right). \quad (10)$$

With Rci_R being Rci at the reference geometry and RCI the geometry parameter that models $Rcep$. From (6), (8) and (10), the referenced based scaling equation of the RCC for a SED with one collector contact is:

$$RCC = RCC_R\left((1-RCX)\left(RCI\frac{W_{ER}L_{ER}}{W_E L_E} + (1-RCI)\frac{W_E L_{ER}}{L_E W_{ER}}\right)\right.$$
$$\left. + RCX\left(1 + GCW\left(\frac{W_E}{W_{ER}}-1\right) + GCL\left(\frac{L_E}{L_{ER}}-1\right)\right)^{-1}\right), \quad (11)$$

where RCC_R is the RCC at the reference geometry and RCX is the geometry parameter, which represents both $Rblx$ and $Rcpl$.
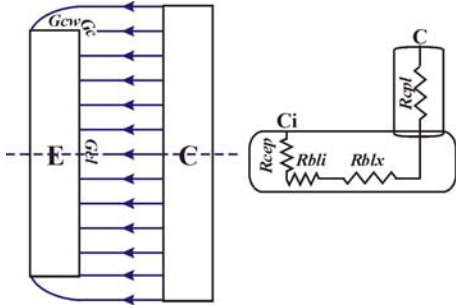
Fig. 2. Top view and cross-section of a SiGe HBT from external (C) to internal collector (Ci) node.

Extending the scaling from SED to MED, the impedance network of the collector resistance from Ci to C is shown in Fig. 3.
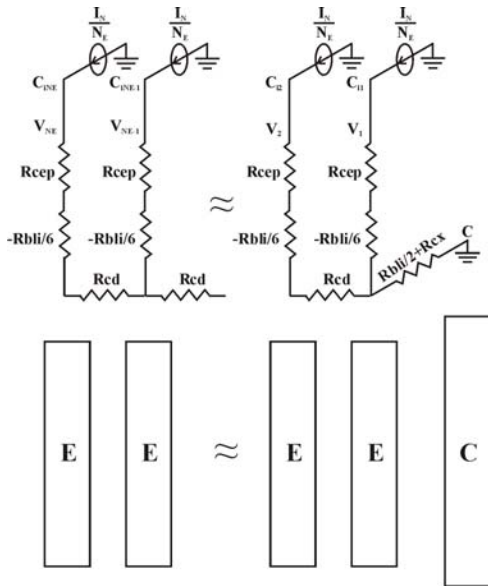
Fig. 3. Top view and collector impedance network of a SED with single collector contact.

If the total current (I_N) is equally distributed among emitter fingers, the internal node voltage V_i can be modeled with an $N_E \times 4$ resistance matrix times four nodal current as:

$$\begin{pmatrix} V_1 \\ V_2 \\ \vdots \\ V_{N_E-1} \\ V_{N_E} \end{pmatrix} = \begin{pmatrix} Rcep & -\dfrac{Rbli}{6} & 0 & \dfrac{Rbli}{2}+Rcx \\ Rcep & -\dfrac{Rbli}{6} & (N_E-1)Rcd & \dfrac{Rbli}{2}+Rcx \\ \vdots & \vdots & \vdots & \vdots \\ Rcep & -\dfrac{Rbli}{6} & \sum_{i=1}^{N_E-2}(N_E-i)Rcd & \dfrac{Rbli}{2}+Rcx \\ Rcep & -\dfrac{Rbli}{6} & \sum_{i=1}^{N_E-1}(N_E-i)Rcd & \dfrac{Rbli}{2}+Rcx \end{pmatrix}\begin{pmatrix} \dfrac{I_N}{N_E} \\ \dfrac{I_N}{N_E} \\ \dfrac{I_N}{N_E} \\ \dfrac{I_N}{N_E} \\ I_N \end{pmatrix} \quad (12)$$

Where $-Rbli/6$ accounts for the distributed effects [9] of the buried collector resistance under emitter so that its effective resistance will become $Rbli/3$ for single collector contact and $Rbli/12$ for double collector contact. Rcd is the buried-layer resistance between two adjacent fingers ($Rblc$) plus $Rbli$. The effective RCC is defined as the average nodal voltage V divided by I_N as:

$$RCC = \frac{V}{I_N} = \frac{V_1+V_2\cdots V_{N_E}}{I_N N_E}$$
$$= \frac{Rcep}{N_E} - \frac{Rbli}{6N_E} + \sum_{i=1}^{N_E-1}i^2\frac{Rcd}{N_E^2} + \frac{Rbli}{2} + Rcx$$
$$= \frac{Rcep}{N_E} + \frac{3N_E-1}{6N_E}Rbli + \frac{(N_E-1)(2N_E-1)}{6N_E}Rcd + Rcx \quad (13)$$
$$= \frac{Rcep}{N_E} + \frac{N_E}{3}Rbli + \frac{(N_E-1)(2N_E-1)}{6N_E}Rblc + Rcx$$

The analysis for the two collector contacts is similar to the single collector contact devices due to the symmetry. In that case, it is sufficient to consider half of the device as shown in Fig. 4, which is half of a MED with odd emitters. Its nodal voltage is modeled using an $(N_E+1)/2 \times 4$ resistance matrix times the node currents as:

$$\begin{pmatrix} V_1 \\ V_2 \\ \vdots \\ V_{\frac{(N_E-1)}{2}} \\ V_{\frac{(N_E+1)}{2}} \end{pmatrix} = \begin{pmatrix} Rcep & -\dfrac{Rbli}{6} & 0 & \dfrac{Rbli}{2}+Rcx \\ Rcep & -\dfrac{Rbli}{6} & \left(\dfrac{N_E}{2}-1\right)Rcd & \dfrac{Rbli}{2}+Rcx \\ \vdots & \vdots & \vdots & \vdots \\ Rcep & -\dfrac{Rbli}{6} & \sum_{i=1}^{\frac{(N_E-3)}{2}}\left(\dfrac{N_E}{2}-i\right)Rcd & \dfrac{Rbli}{2}+Rcx \\ Rcep & -\dfrac{Rbli}{6} & \sum_{i=1}^{\frac{(N_E-1)}{2}}\left(\dfrac{N_E}{2}-i\right)Rcd & \dfrac{Rbli}{2}+Rcx \end{pmatrix}\begin{pmatrix} \dfrac{I_N}{N_E} \\ \dfrac{I_N}{N_E} \\ \dfrac{I_N}{N_E} \\ \dfrac{I_N}{N_E} \\ \dfrac{I_N}{2} \end{pmatrix} \quad (14)$$

By averaging the node voltages, the RCC for an odd emitter with two collector contacts device is:

$$RCC = \frac{V}{I_N} = \frac{2\left(V_1 + V_2 \cdots V_{(N_E-1)/2}\right) + V_{(N_E+1)/2}}{I_N N_E}$$

$$= \frac{Rcep}{N_E} + \frac{3N_E - 2}{12N_E}Rbli + \frac{(N_E-1)(N_E-2)}{12N_E}Rcd + \frac{Rcx}{2} \quad (15)$$

$$= \frac{Rcep}{N_E} + \frac{N_E}{12}Rbli + \frac{(N_E-1)(N_E-2)}{12N_E}Rblc + \frac{Rcx}{2}$$
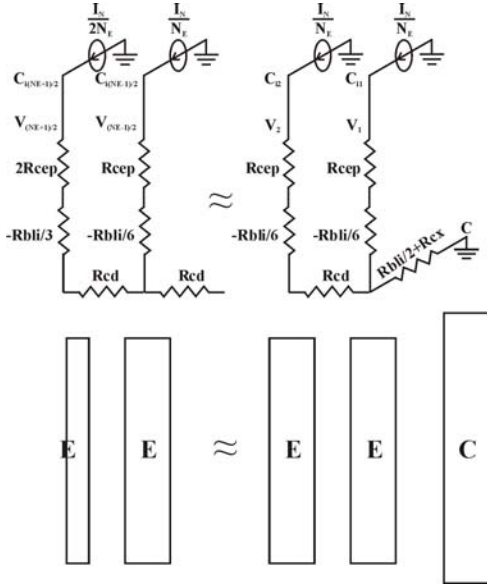
Fig. 4. Top view and collector impedance network of an odd-emitter, two collector contacts device.

For even number of emitters, its internal nodal voltages are the same as for the single collector contact with half of its emitter fingers and total nodal current. Its collector resistance will be:

$$RCC = \frac{Rcep}{N_E} - \frac{Rbli}{6N_E} + 2\sum_{i=1}^{\frac{N_E}{2}-1} i^2 \frac{Rcd}{N_E^2} + \frac{Rbli}{4} + \frac{Rcx}{2}$$

$$= \frac{Rcep}{N_E} + \frac{3N_E-2}{12N_E}Rbli + \frac{(N_E-1)(N_E-2)}{12N_E}Rcd + \frac{Rcx}{2} \quad (16)$$

$$= \frac{Rcep}{N_E} + \frac{N_E}{12}Rbli + \frac{(N_E-1)(N_E-2)}{12N_E}Rblc + \frac{Rcx}{2}.$$

It happens that the scaling equations for double collector, odd and even emitter devices are the same. RCC from (13), (15) and (16) can be expressed as a single analytical equation with the number of collector contact (N_C) as:

$$RCC = \frac{Rcep}{N_E} + \frac{N_E}{3N_C^2}Rbli + \frac{(N_E-1)(2N_E/N_C^2-1)}{6N_E}Rblc + \frac{Rcx}{N_C} \quad (17)$$

From (11) and (17), the reference based scaling equation of the RCC for the SED and MED with different N_C is combined as a single expression as:

$$RC1 = (1-RCX)\left(\frac{RCI}{N_E}\frac{W_{ER}L_{ER}}{W_E L_E} + \frac{N_E}{N_C^2}(1-RCI)\frac{W_E L_{ER}}{W_{ER}L_E}\right),$$

$$RC2 = \frac{(N_E-1)(2N_E/N_C^2-1)}{6N_E}RCXC\frac{W_D L_{ER}}{W_{DR}L_E},$$

$$\quad (18)$$

$$RC3 = \frac{RCX}{N_C}\left(1 + \frac{N_E}{N_C}GCW\left(\frac{W_E}{W_{ER}}-1\right) + GCL\left(\frac{L_E}{L_{ER}}-1\right)\right)^{-1},$$

$$RCC = RCC_R(RC1 + RC2 + RC3).$$

Where RCXC is the geometry parameter that models the *Rblc*.

III. MODEL IMPLEMENTATION AND PARAMETER EXTRACTION IN IC-CAP

Based on the scaling equations derived in section II and the previous geometry scaling results [6], the configuration scalable model is utilized as extension of the standard Mextram model implemented in Verilog-A [10] as following:

```
`include "frontdef.inc"
`define  SELFHEATING
`define  SUBSTRATE

module bjt504t_va (c, b, e, s, dt);

// External ports
     inout c, b, e, s, dt;
     electrical c, b, e, s, dt;

// Internal nodes
     electrical e1, b1, b2, c1, c2;
     electrical noi;

`include "parameters.inc" // Add new instant and
geometry parameters  in this module.
`include "variables.inc" // Add new variables  in
this module.
analog begin
`include  "geo_scaling.inc" // Geometry scaling
equations are added in this module.
`include "initialize.inc"
`include "tscaling.inc"
`include "evaluate.inc"
end
endmodule
```

In the implemented model, new instance parameters (NE, NC, WE and LE) and geometry parameters (RTHA, RTHW…) are added in the module "parameters.inc" to account for the layout configuration and geometry scaling of the bipolar devices. The geometry scalable Mextram model parameters (RTH, RCC…) in "parameters.inc" are used as the reference parameters. The scaling

equations for the scalable Mextram model parameters listed in Table I are implemented in "geo_scaling.inc". The geometrical quantities (WB, LB, WC, and LC) in Table I, representing the size of active region and collector-substrate junction, can be scaled with WE and LE based on the design rule of the specific process. Some new variables are added in the module "variables.inc" and used in the module "geo_scaling.inc" for the geometry scaled results of the scaling equations. They will replace the scalable model parameters in the temperature-scaling module "tscaling.inc", which the results that will be used later in the main module "evaluate.inc". As a result, the geometry, configuration and temperature scaling of the bipolar transistor are taken into account in the model evaluation.

TABLE I
SCALING EQUATIONS FOR MULTI-FINGER DEVICES

Scalable Parameters	Geometry Dependent	Finger Dependent
IS, IK, IBF, IBR	W_E, L_E	N_E
CJE, CJC, IHC	W_E, L_E	N_E
ISS, IKS	W_B, L_B	N_E
CJS	W_C, L_C	N_E
BF, VEF, VER	W_E, L_E	none
PE, PC, TAUB	W_E, L_E	none
BRI	W_E, L_E	none
PS	W_C, L_C	none
RE, RCV, SCRCV	W_E, L_E	$1/N_E$
RBV	W_E, L_E	$1/N_E$
RBC	W_E, L_E	$1/N_E$
RTH	W_B, L_B	(5)
RCC	W_E, L_E	(18)

An extension of the unified parameter extraction procedure for the scalable Mextram model is implemented in an Agilent IC-CAP model file and using high speed SiGe HBTs [11] as a test example. The extraction procedure starts at a selected reference geometry device from the available geometry matrix. The reference parameters are extracted at the Device Under Test (DUT) "npn_ref" from the reference geometry following standard procedure [12] going from low injection towards high injection related parameters. The temperature scaling parameters are extracted in DUT "temp_scaling" before high injection parameters extraction to accurately model the temperature rise from self-heating effect at high current region. Following the high current parameters extraction, extraction of geometry parameters in DUT "geom_scaling" is performed. After geometry parameters extraction, a DUT "conf_scaling" is added for RTHC and RCXC extraction from measured output characteristic of MEDs.

The essential feature of the proposed geometry and configuration scaling methodology is a direct extraction of the geometry parameters from the measured electrical characteristics and the model parameters as reference parameters are extracted only once for a single reference geometry. The MEDs are used for RTHC and RCXC extraction. Without re-extracting any parameter from SEDs after RTHC and RCXC extraction, Fig. 5 shows the model simulated (in solid lines) unity gain bandwidth (f_T) vs. collector current (I_C) from ADS [13] comparing with the measured data (in circles) from N_E =1~4, N_C =2 and different A_E. The model simulation results can accurately predict f_T degradation with increasing emitter finger number but the default Mextram model parameter "MULT" scaling results (in dashed line), which puts MULT SEDs in parallel, is not able to do that. Since the f_T can be simply expressed as a sum of the total forward transit time (τ_F), base-emitter junction capacitance (C_{je}), base-collector junction capacitance (C_{jc}) and RCC as [14]:

$$\frac{1}{2\pi f_T} = \tau_F + \frac{kT}{qI_C}\left(C_{je} + C_{jc}\right) + RCC \cdot C_{jc}, \quad (19)$$

the accurate prediction of f_T degradation with N_E from our model validates the thermal resistance and collector resistance scaling results.

IV. CONCLUSIONS

In this paper, the reference geometry based scaling approach for Mextram model has been extended to different layout configuration of bipolar devices. The proposed scaling methodology employs effective thermal and collector node assumption.

The configuration scalable model uses almost the same set of the model parameters as in the geometry scalable model except RTHC and RCXC, which model the mutual heating effect and collector resistance between two adjacent fingers and two additional instance parameters N_E and N_C for different layout configurations. The model nicely predicts the f_T degradation due to increase of mutual heating and the collector delay time with increasing N_E. It is concluded that the number of emitters can't be increased without a limit as for emitter area.
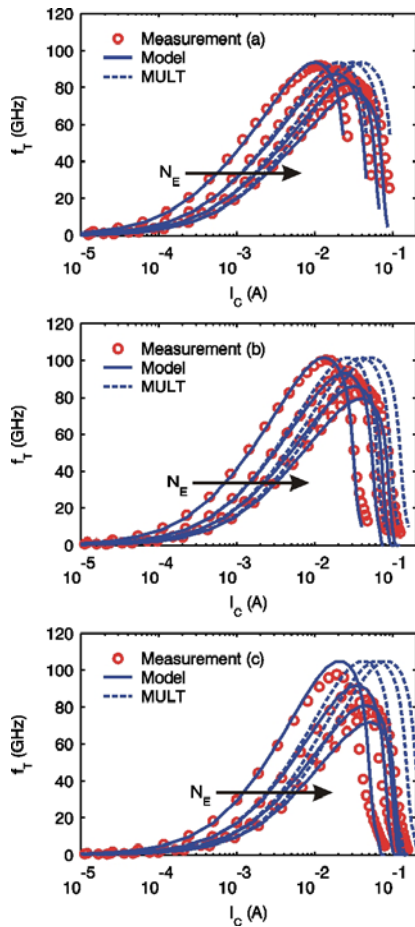
Fig. 5 model simulation and measurement results of f_T vs. I_C from (a) $A_E = 0.2 \times 10.16$ (b) $A_E = 0.3 \times 10.16$ and (c) $A_E = 0.6 \times 10.16$ μm^2 with $N_E = 1\sim4$, $N_C = 2$ at $V_{CB} = 1V$.

REFERENCES

[1] T. Hashimoto et al., "Direction to improve SiGe BiCMOS technology featuring 200-GHz SiGe HBT and 80-nm gate CMOS," IEEE International Electron Devices Meeting, pp. 5.5.1 - 5.5.4, 2003.

[2] M.W. Hsieh et al., "Frequency response improvement of 120 GHz f_T SiGe HBT by optimizing the contact configurations," IEEE MTT-S International Microwave Symposium, pp. 967 - 970, Jun. 2004.

[3] J. C. J. Paasschens, W. J. Kloosterman, "The Mextram Bipolar Transistor Model - Level 504," Nat. lab. Unclassified Report, Koninklijke Philips Electronics N.V. 2001.

[4] C. T. Kirk, "A theory of transistor cut-off frequency (f_T) fall-off at high current densities, " IRE Trans. Electron Devices, vol. 9, pp.164-174, 1962.

[5] H. C. de Graaff and W. J. Kloosterman, "Modeling of the Collector Epilayer of a Bipolar Transistor in the MEXTRAM Model," IEEE Trans. Electron Devices, vol. 42, pp.274-282, Feb. 1995.

[6] H.-C. Wu, S. Mijalkovic and J.N. Burghartz," A Unified Parameter Extraction Procedure for Scalable Bipolar Transistor Model Mextram," Proc. NSTI Nanotech 2006, Vol. 3, pp. 872-875.

[7] "IC-CAP 2004," Agilent Technology.

[8] M. Latif and P.R. Bryant, "Network Analysis Approach to Multidimensional Modeling of Transistors Including Thermal Effects," IEEE Transactions on Computer-Aided Design of Integrated Circuits and Systems, pp. 94 - 101, Apr. 1982.

[9] J. C. J. Paasschens, "Modeling distributed resistance effect," Private Communication.

[10] H.-C. Wu, S. Mijalkovic and J.N. Burghartz, "Mixed Compact and Behavior Modeling Using AHDL Verilog-A," 2003 IEEE International Workshop on Behavioral Modeling and Simulation (BMAS 2003), pp. 139-143.

[11] J.C.-H. Lin et al., "State of Art RF/Analog Foundry Technology," IEEE Bipolar/BiCMOS Circuits and Technology Meeting, pp. 73-79. 2002.

[12] J. C. J. Paasschens, W. J. Kloosterman and R.J. Havens, "Parameter Extraction for the Bipolar Transistor Model Mextram - Level 504," Nat. lab. Unclassified Report, Koninklijke Philips Electronics N.V. 2001.

[13] "Advanced Design System 2005A," Agilent Technology.

[14] T. E. Idleman, F. S. Jenkins, W. J. McCalla and D. O. Pederson, "SLIC- A Simulator for Linear Integrated Circuits," IEEE J. Solid-State Circuits, pp. 188 - 203, Aug. 1971.